Int J Adv Manuf Technol (2018) 95:961–972
https://doi.org/10.1007/s00170-017-1283-0

ORIGINAL ARTICLE

Chatter detection based on synchrosqueezing transform and statistical indicators in milling process

Hongrui Cao[1] · **Yiting Yue**[1] · **Xuefeng Chen**[2] · **Xingwu Zhang**[1]

Received: 27 July 2017 / Accepted: 26 October 2017 / Published online: 7 November 2017

Abstract Chatter is a self-excited vibration between the workpiece and tool. In view of the non-stationarity of the chatter signal, the synchrosqueezing transform (SST) is used to process vibration signals during cutting, which can enhance the energy ratio of chatter. In order to eliminate the interference of tooth passing frequency and its harmonics, a time-frequency filtering method is applied to filter these frequency components out. Then, the vibration signal is reconstructed by inverse SST and statistical indexes in time and frequency domains are calculated. The cutting tests are carried out to select statistical indexes which are sensitive to chatter. The effectiveness of the proposed method is verified with cutting tests, and the results show that the chatter can be detected successfully before severe chatter marks are left on the workpiece.

Keywords Chatter detection · Statistical indicators · Time-frequency filtering · Synchrosqueezing transform

1 Introduction

Chatter is the self-excited vibration of the tool-workpiece system, affecting the improvement of machining precision and efficiency. In the high-speed machining process of complex parts, the damping effect in the cutting process is weakened, which makes the chatter more likely to occur than the low-speed cutting [1, 2]. The chatter problem has become a bottleneck in restricting machining precision and efficiency [3–6]. In order to solve the problem of chatter in high-speed machining process, it is of great theoretical significance and application value to study the early chatter detection methods, which will effectively promote the development of intelligent machine tool and manufacture [7].

The key issue of chatter detection is to process the online measured signals and extract the sensitive indicators to reflect the chatter occurrence. Therefore, how to choose the most appropriate method from a variety of signal processing methods and extract the most sensitive features have been the focus of many research. When the chatter occurs, the vibration of the tool-workpiece system is strengthened in the time domain, so the statistics feature in time domain is widely used for chatter detection. From another point of view, when chatter occurs, the frequency components of the measured signals will change and some new frequency components will appear near the natural frequency of the system. Therefore, it is common to detect chatter in the frequency domain according to the change of the frequency components [8, 9]. Due to the nonstationary properties of the measured signals in machining processes, the signal processing methods in time-frequency domain attract more attentions. The information in both time and frequency domains can be combined together to achieve better results. So far, the time-frequency (TF) analysis method applied to machine chatter monitoring mainly includes short-time Fourier transform (STFT) [10], continuous wavelet transform (CWT) [11–13], wavelet transform [14–18], empirical mode decomposition (EMD) [19–21], and local mean decomposition (LMD) [22].

Due to the constraints of Heisenberg's uncertainty principle, the time and frequency resolutions in traditional TF analysis are limited. Aiming at high resolution in TF plane, Daubechies et al. [23] proposed a new time-frequency

✉ Hongrui Cao
chr@mail.xjtu.edu.cn

[1] Key Laboratory of Education Ministry for Modern Design and Rotor-Bearing System, Xi'an Jiaotong University, Xi'an 710049, China

[2] State Key Laboratory for Manufacturing Systems Engineering, Xi'an Jiaotong University, Xi'an 710049, China

rearrangement method—synchrosqueezing transform (SST), which greatly improves the time-frequency aggregation based on the original time-frequency results. In our previous work [24], the SST was used to analyze the sound signals recorded with the microphone and a time-frequency representation is obtained. The singular value decomposition (SVD) method was employed to condense the TF matrix, and the first-order singular value was calculated as the chatter indicator. In this paper, the vibration signals are measured and then processed with SST. In order to eliminate the interference of tooth passing frequency and its harmonics, a time-frequency filtering method is applied and then, the filtered signal is reconstructed by inverse SST. After that, statistical indicators in time and frequency domains are calculated to detect chatter.

2 Signal preprocessing based on synchrosqueezing transform

SST is mostly based on STFT or CWT as the preliminary TF processing method, and an important characteristic of CWT is that the time or frequency resolution is different in the high and low frequency bands. Therefore, the TF distribution of the chatter frequencies at different band positions will be different if CWT is used for the initial TF processing. When SST is performed subsequently, the frequency resolution of different bands is different, and the effect of energy aggregation and rearrangement on the theoretical center frequency will be also different. Considering the feature extraction based on the whole TF distribution in the later stage, if the index is extracted based on different frequency bands, it may affect the uniformity of the benchmarks and cannot guarantee the calculation and comparison in the same scale. Therefore, the SST based on STFT is more suitable for chatter detection because of its uniform time-frequency resolution.

2.1 Brief overview of synchrosqueezing transform

The principle and calculation method of STFT-based synchrosqueezing transform are as follows.

For a given single component harmonic signal $x(t) = A\cos(\omega_0 t)$, the TF distribution of STFT $S_x(u, \xi)$ is obtained from the Plancherel theorem as Eq. (1).

$$\begin{aligned} S_x(u,\xi) &= \frac{1}{2\pi}\int_{-\infty}^{+\infty}\hat{x}(\omega)\hat{g}(\omega-\xi)e^{j\omega u}d\omega \\ &= A\int_{-\infty}^{+\infty}\delta(\omega-\omega_0)\hat{g}(\omega-\xi)e^{j\omega u}d\omega \\ &= A\hat{g}(\omega_0-\xi)e^{j\omega_0 u} \end{aligned} \tag{1}$$

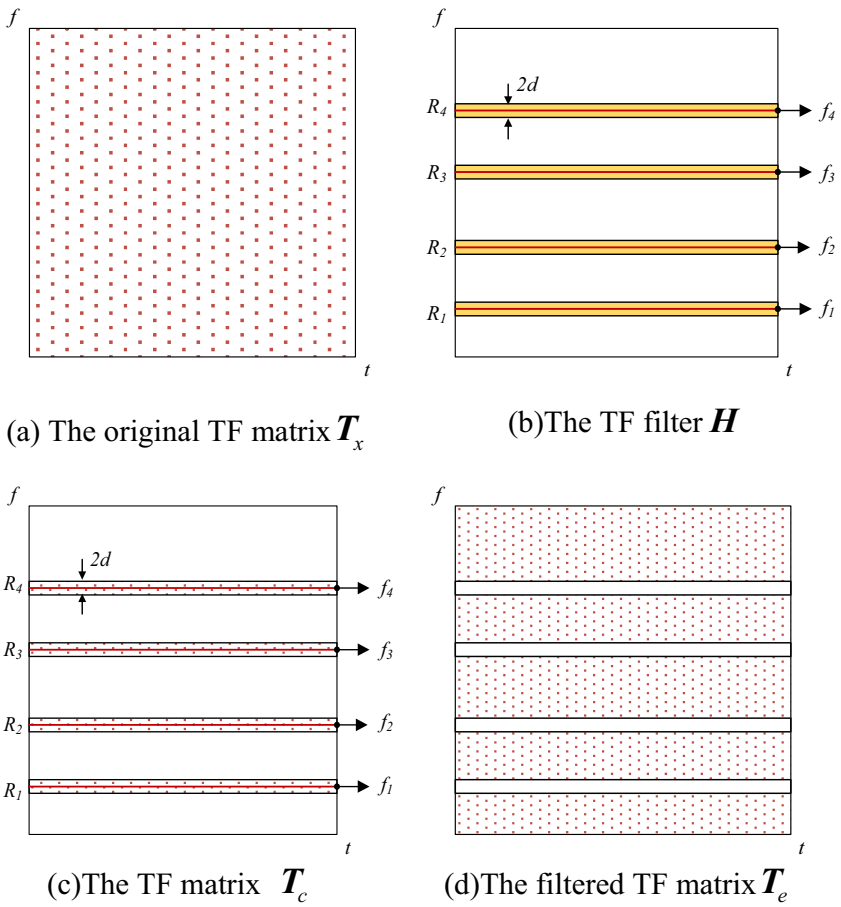

Fig. 1 The sketch of TF filtering method based on SST. **a** The original TF matrix $\boldsymbol{T}_x$. **b** The TF filter $\boldsymbol{H}$. **c** The TF matrix $\boldsymbol{T}_c$. **d** The filtered TF matrix $\boldsymbol{T}_e$

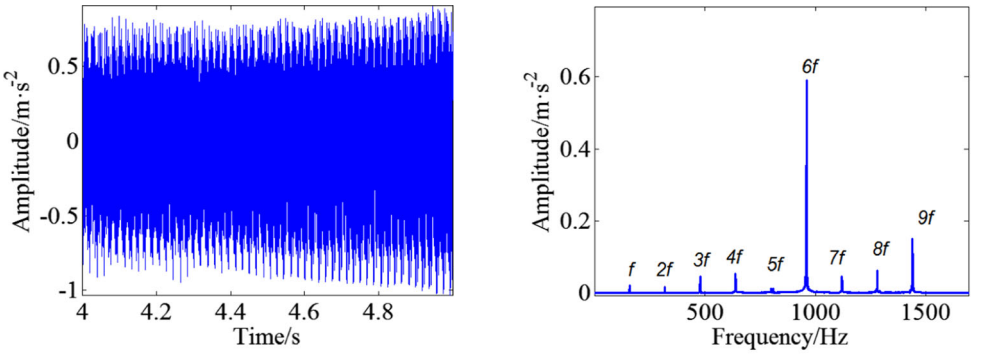

(a) The waveform in time domain (b) The spectrum in frequency domain

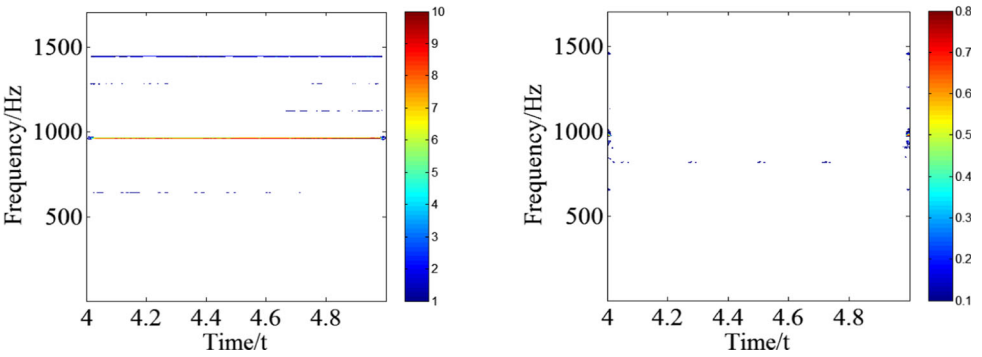

(c) The TF distribution before filtering (d) The TF distribution after filtering

Fig. 2 The result of TF filtering method. **a** The waveform in time domain. **c** The spectrum in frequency domain. **c** The TF distribution before filtering. **d** The TF distribution after filtering

where $\hat{x}(\omega)$ and$\hat{g}(\omega-\xi)$ are the Fourier transform of $x(t)$- and a Gaussian window functiong$(t-\mu)$, μ is the time-shifting variable, and ξ is the frequency shifting variable of$g(t)$.

Then, the time-shift partial derivative of $S_x(u,\xi)$is calculated with Eq. (2).

$$\partial_u S_x(u,\xi) = A\hat{g}(\omega_0-\xi)e^{j\omega_0 u} \times j\omega_0 = j\omega_0 \times S_x(u,\xi) \quad (2)$$

Table 1 Statistical characteristic quantity in time domain

Dimensional indicators	Expression	Dimensionless indicators	Expression
Mean value	$\bar{x} = \frac{1}{N}\sum_{n=1}^{N} x_e$	Waveform index	$SF = \frac{X_{\text{rms}}}{X_a}$
Variance	$\sigma^2 = \frac{1}{N}\sum_{n=1}^{N}(x_e-\bar{x})^2$	Peak index	$CF = \frac{\max\lvert x_e\rvert}{X_{\text{rms}}}$
Root mean square value	$X_{\text{rms}} = \sqrt{\frac{1}{N}\sum_{n=1}^{N} x_e^2}$	Impulse index	$IF = \frac{\max\lvert x_e\rvert}{X_a}$
Root square amplitude	$X_s = \left(\frac{1}{N}\sum_{n=1}^{N}\sqrt{\lvert x_e\rvert}\right)^2$	Margin index	$CLF = \frac{\max\lvert x_e\rvert}{X_s}$
Absolute mean amplitude	$X_a = \frac{1}{N}\sum_{n=1}^{N}\lvert x_e\rvert$	Skewness index	$S = \frac{\sum_{n=1}^{N}\lvert x_e-\bar{x}_e\rvert^3}{(N-1)\sigma^3}$
Peak-to-peak value	$X_p = \max(x_e) - \min(x_e)$	Kurtosis index	$K = \frac{\sum_{n=1}^{N}\lvert x_e-\bar{x}_e\rvert^4}{(N-1)\sigma^4}$

Table 2 Statistical characteristics in frequency domain

Statistical indicators	Expression	Statistical indicators	Expression
P_{13}	$P_{13}=\sum_{k=1}^{K}\left(s_e-\frac{1}{k}\sum_{k=1}^{k}s_e\right)^{\frac{2}{K-1}}$	P_{20}	$P_{20}=\frac{\sum_{k=1}^{K}f_k{}^2s_e}{\sqrt{\sum_{k=1}^{K}s_e\sum_{k=1}^{K}f_k{}^4s_e}}$
P_{16}	$P_{16}=\frac{\sum_{k=1}^{K}f_ks_e}{\sum_{k=1}^{K}s_e}$	P_{21}	$P_{21}=\frac{P_{17}}{P_{16}}$
P_{17}	$P_{17}=\frac{\sum_{k=1}^{K}(f_k-P_{16})^2s_e}{K}$	P_{23}	$P_{23}=\frac{\sum_{k=1}^{K}(f_k-P_{16})^4s_e}{KP_{17}^4}$
P_{19}	$P_{19}=\sqrt{\frac{\sum_{k=1}^{K}f_k{}^4s_e}{\sum_{k=1}^{K}f_k{}^2s_e}}$	P_{24}	$P_{24}=\frac{\sum_{k=1}^{K}\sqrt{(f_k-P_{16})s_e}}{K\sqrt{P_{17}}}$

If $S_x(u,\xi)\neq 0$, the instantaneous frequency (IF) can be estimated by Eq.(3).

$$\omega_0=\frac{\partial_u S_x(u,\xi)}{jS_x(u,\xi)} \tag{3}$$

The above equation shows that the ratio of the partial derivative of the STFT result to the STFT result itself can reflect the intrinsic frequency information of the signal to be analyzed. This ratio is called the IF estimation operator, i.e., the frequency shift operator$\tilde{\omega}_x$, as shown in Eq. (4).

$$\tilde{\omega}_x(u,\xi)=\frac{\partial_u S_x(u,\xi)}{jS_x(u,\xi)} \tag{4}$$

The rearrangement formula is given as Eq. (5) and the reconstitution formula is given as Eq. (6) according to the reconstitution nature of STFT.

$$T_{x,S}(u,\omega)=\int S_x(u,\xi)\delta\left(\omega-\tilde{\omega}_x(u,\xi)\right)d\xi \tag{5}$$

$$x(u)=\frac{1}{2\pi g(0)}\int T_{u,S}(u,\omega)d\omega \tag{6}$$

2.2 TF filtering method based on SST

Although new frequency components emerge in the spectrum of the signal in chatter state, the tooth passing frequency and its harmonics dominate in the early stages of

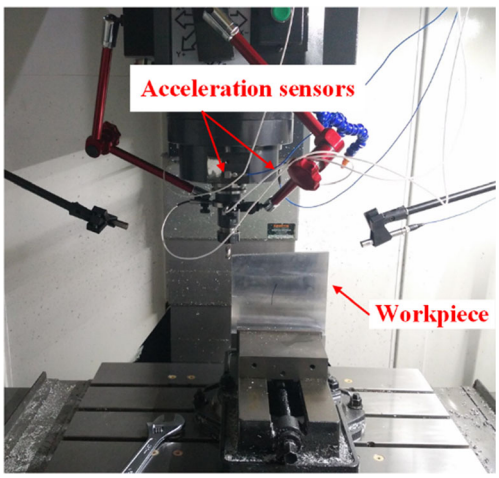

Fig. 3 The experimental setup

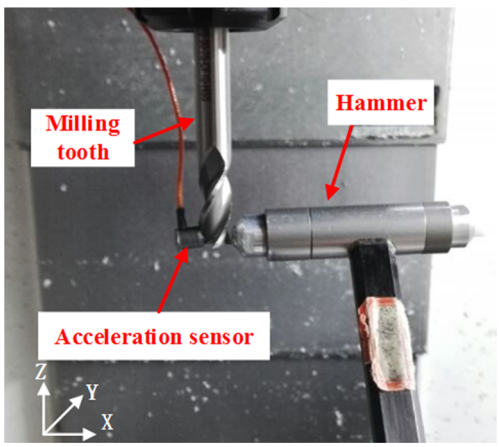

Fig. 4 The experimental setup of FRF test

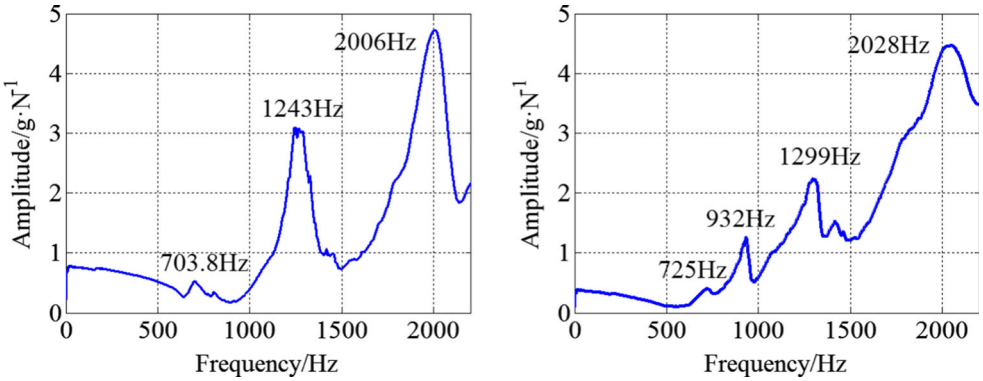

Fig. 5 FRFs of the STT system. a X direction. b Y direction

transition. Thus, the chatter frequency components are easily to be submerged. If the chatter indexes are only extracted from the frequency spectrum, the changes of indicators may not be obvious, lagging the detection time of chatter. Therefore, the signal should be filtered, and the forced vibration frequencies will be filtered out to eliminate their interference on the extraction of chatter frequencies. Thus, the weak chatter frequency and the relative proportion of chatter components can be enhanced for the subsequent indicator extraction.

In this paper, a TF filtering method based on SST is presented. Some fixed frequency components are directly filtered out from the time-frequency distribution to obtain the remaining time-frequency information. The specific algorithm for this TF filtering is described below:

(1) Construct a time-frequency filter$\boldsymbol{H}[m,n]$with the same size as the time-frequency matrix to be filtered$\mathbf{T}_x[m,n]$, where m and n represent the frequency and time order numbers, respectively. In this time-frequency filter, according to the location. In this timefrequency filter, the TF zone R with the center frequency f_c and bandwidth $2d$ is constructed according to the location of the selected frequency components. The time-frequency coefficients in this zone are 1 and the other time-frequency coefficients outside are 0, as shown in Eq. (7).

$$\boldsymbol{H}[m,n] = \begin{cases} 1 & [m,n] \in R \\ 0 & [m,n] \notin R \end{cases} \tag{7}$$

(2) Do multiplication of corresponding elements in the TF matrix$\boldsymbol{T}_x[m,n]$ and the TF filter $\boldsymbol{H}[m,n]$, as shown in Eq. (8), which makes the TF coefficients in matrix $\boldsymbol{T}_x$ correspond to the location of R multiplied by 1 and other coefficients in matrix $\boldsymbol{T}_x$ are multiplied by 0. In this way, only some specific frequency band components $f_c \pm d$ in $\boldsymbol{T}_x$ are reserved and the new TF matrix $\boldsymbol{T}_c$is obtained:

$$\boldsymbol{T}_c[m,n] = \boldsymbol{T}_x[m,n] \odot \boldsymbol{H}[m,n] \tag{8}$$

where $\odot$ means the multiplication of corresponding elements of two matrixes with the same size.

(3) Subtracting$\boldsymbol{T}_c$from the original time-frequency matrix$\boldsymbol{T}_x$to obtain a new time-frequency matrix$\boldsymbol{T}_e$that filters out the

Table 3 Experimental parameters of four milling states

Milling states	Spindle speed (r/min)	Feedrate (mm/min)	Width of cut (mm)	Depth of cut (mm)
Stable milling	8500	1500	20	1
Chatter transition phase I	8500	1500	20	2
Chatter transition phase II	8500	1500	20	3
Severe chatter	8500	1500	20	5

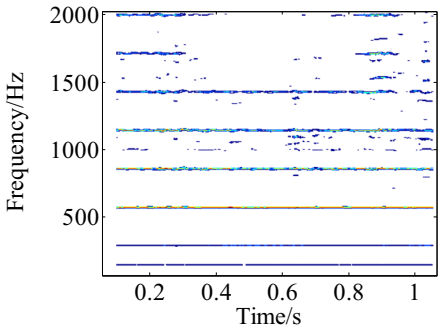

(a)TF distribution in stable milling

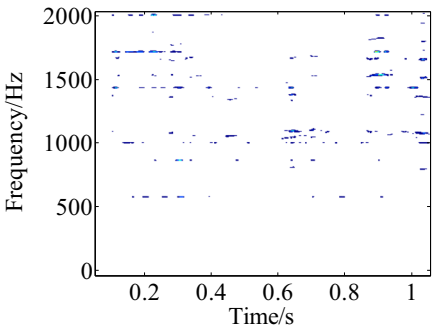

(b) The filtered TF distribution in stable milling

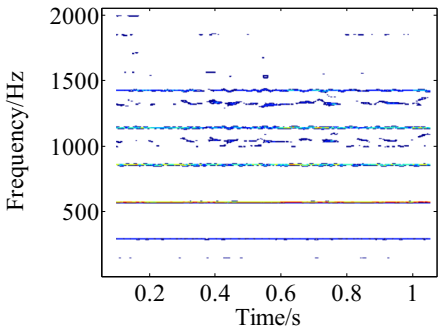

(c) TF distribution in transition phase I

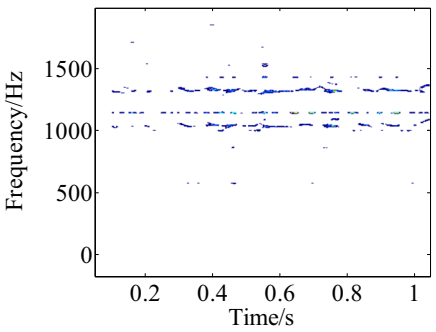

(d) The filtered TF distribution in transition phase I

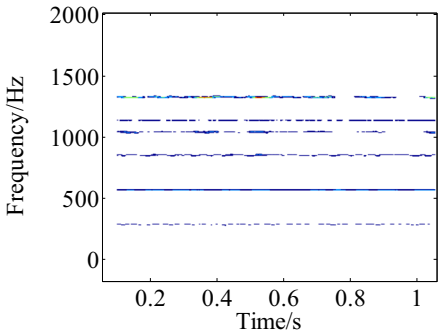

(e) TF distribution in transition phase II

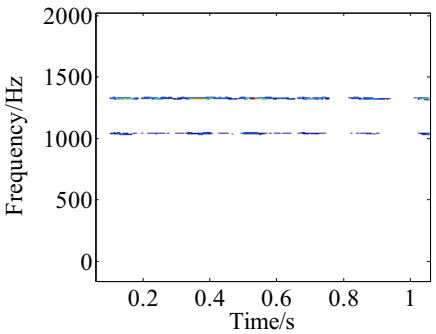

(f) The TF filtered distribution in transition phase II

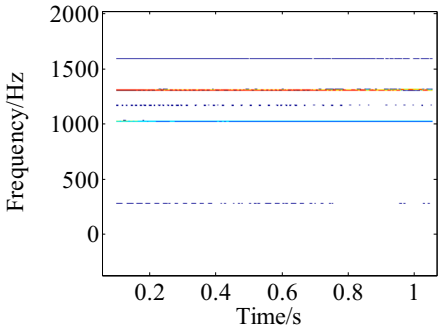

(g) TF distribution in severe chatter

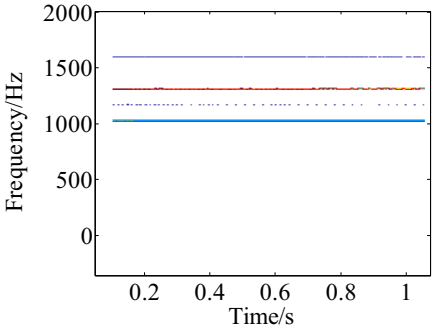

(h) The filtered TF distribution in severe chatter

◀ **Fig. 6** TF distributions and the filtered TF distributions of four different milling states. **a** TF distribution in stable milling. **b** The filtered TF distribution in stable milling. **c** TF distribution in transition phase I. **d** The filtered TF distribution in transition phase I. **e** TF distribution in transition phase II. **f** The TF filtered distribution in transition phase II. **g** TF distribution in severe chatter. **h** The filtered TF distribution in severe chatter

frequency band $f_c \pm d$ and retains other time-frequency components, which is similar to the bandstop filter.

As shown in Fig. 1, the multiple frequency components f_1, f_2, f_3, and f_4 are filtered out from the original TF distribution, and the remaining time-frequency parts are retained for further analysis.

The vibration signal in stable cutting process and its spectrum are shown in Fig. 2a and b, respectively, where the basic frequency f and its harmonic frequencies have been marked out. The original milling signal is processed by SST to obtain the unfiltered TF distribution as shown in Fig. 2c. Then, a TF filter is constructed with a series of TF zones where the basic frequency f and its harmonic frequencies are the central frequency and the filtering of TF distribution is performed, as shown in Fig. 2d. It can be found that the basic frequency and its harmonic frequencies are nearly filtered, which proves the effectiveness of TF filtering method.

3 Statistical indicators in time and frequency domains

3.1 Time-frequency reconstruction of the signal

In comparison with the traditional time-frequency rearrangement method, the SST only rearranges the coefficients in the frequency direction, so it is reversible. The vibration signal can be reconstructed after time-frequency filtering, which can provide the basis for indicator extraction in time domain and frequency domain.

The steps of reconstruction of SST are shown as follows:

1) For the measured signal $x(t)$, the time-frequency distribution $\boldsymbol{T}_x$ is obtained according to rearrangement algorithm of SST.
2) Time-frequency filtering is applied to TF distribution $\boldsymbol{T}_x$, so that the forced vibration components (i.e., tooth

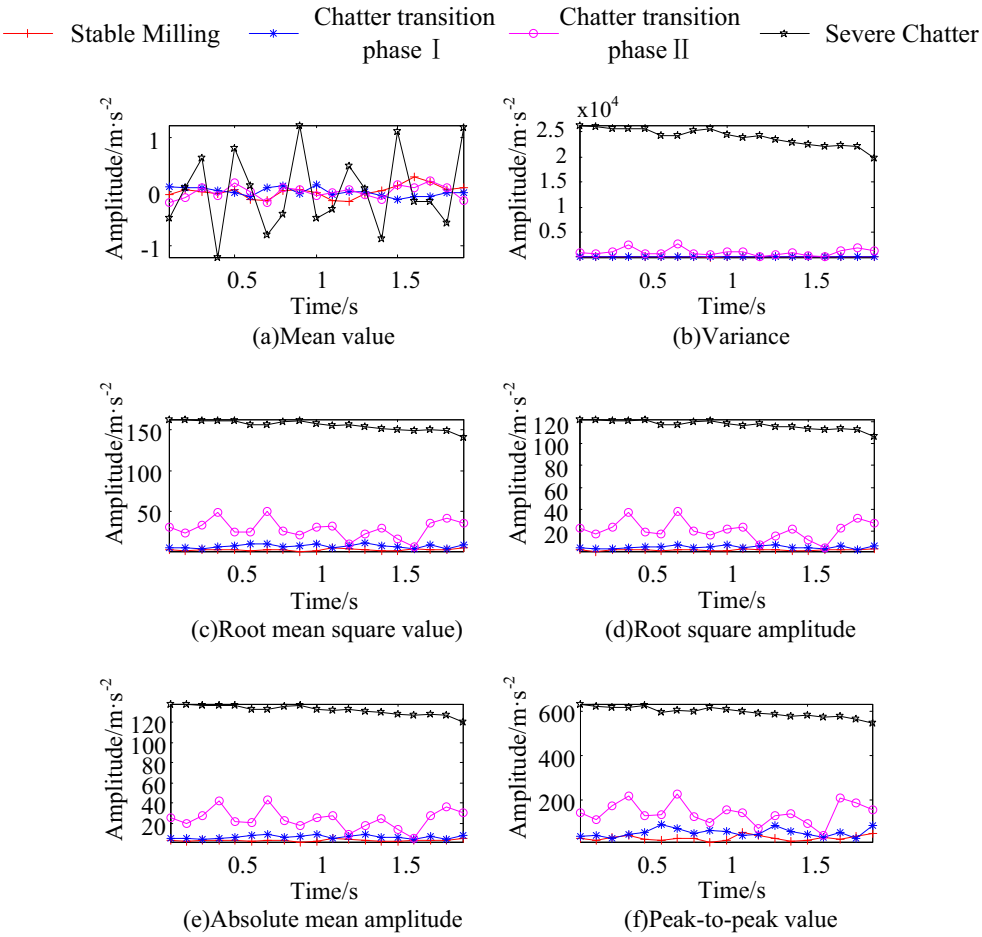

Fig. 7 Dimensional statistical indexes of the reconstructed signals in time domain. **a** Mean value. **b** Variance. **c** Root mean square value. **d** Root square amplitude. **e** Absolute mean amplitude. **f** Peak-to-peak value

passing frequency and its harmonic frequencies) can be filtered out and a new time-frequency matrix $\boldsymbol{T}_e$ is obtained.

3) Inverse transformation is carried out on time-frequency matrix $\boldsymbol{T}_e$ according to Eq. (6) to reconstruct a new signal $x_r(t)$.

3.2 Statistical indicators of the reconstructed signal in time domain

After time-frequency filtering and reconstruction, the new signal is mainly composed of noise components in the stable milling state. When chatter occurs, the amplitude in time domain will increase rapidly in a short time. This change can be quantitatively analyzed by the statistical feature extraction of the signal in time domain.

The commonly used time domain statistical indicators include dimensional indicators, such as variance, mean square value, and peak-to-peak value, as well as non-dimensional indicators, such as waveform indicators and kurtosis indicators. Dimensional indicators have the advantage of reflecting the amplitude and energy changes of the vibration signal in the time domain. For example, the mean value can reflect the changing trend of the signal center, and the peak-to-peak value can reflect vibration intensity of the signal. However, the dimensional indexes are easily to be affected by cutting parameters (cutting speed, feed rate, etc.). The dimensionless indexes are generally calculated on the ratio of the dimension indexes, which are not likely to be affected by the working condition and have little effect on the result when the measuring point is slightly changed.

The commonly used statistical indexes in time domain are shown in Table 1, where $x_e(n)$ represents the reconstructed signal, and N is the data length ($n = 1, 2, \cdots, N$).

3.3 Statistical indicators of the reconstructed signal in frequency domain

The new time domain signal obtained by synchrosqueezing reconstruction in the stable milling state is mainly composed of noise components, and the frequency distribution is dispersed. When the chatter occurs, there will be new chatter frequencies near the natural frequency of the system. The position of main energy peak moves from high frequency to low frequency in frequency spectrum, and finally concentrated on the chatter frequency. In addition, the main frequency band becomes narrower as the degree of dispersion reduced. Therefore, the change from stable cutting to chatter can be

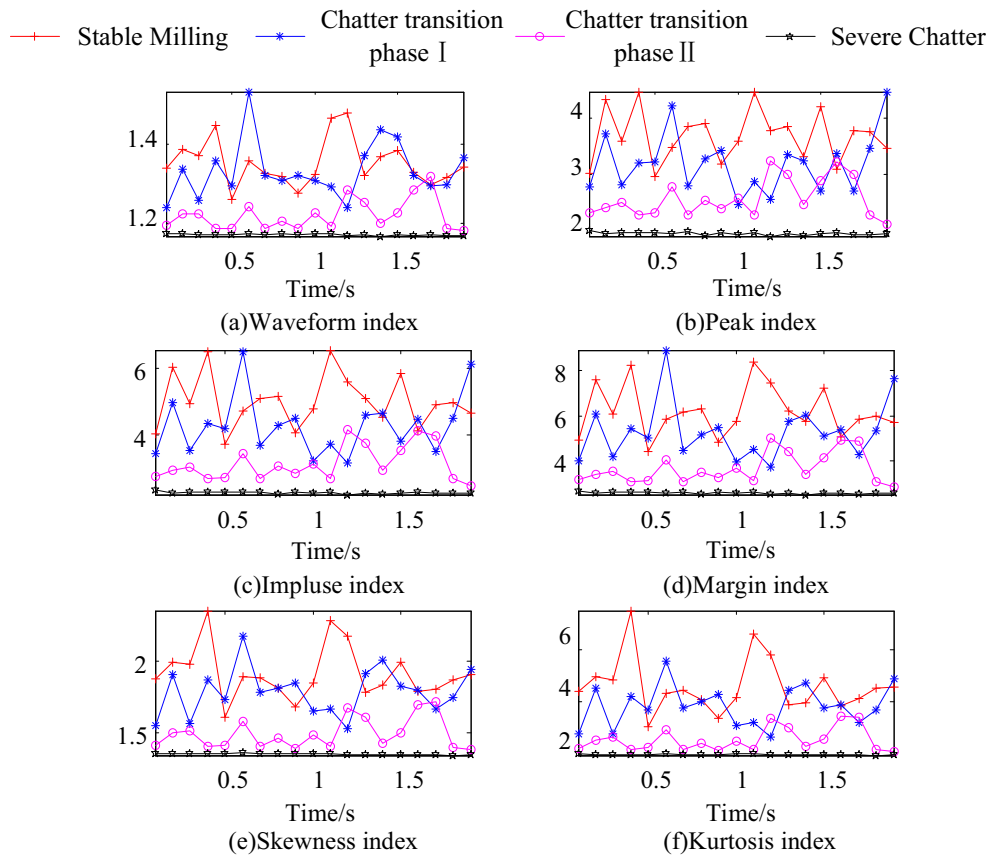

Fig. 8 Dimensionless statistical indexes of the reconstructed signals in time domain. **a** Waveform index. **b** Peak index. **c** Impulse index. **d** Margin index. **e** Skewness index. **f** Kurtosis index

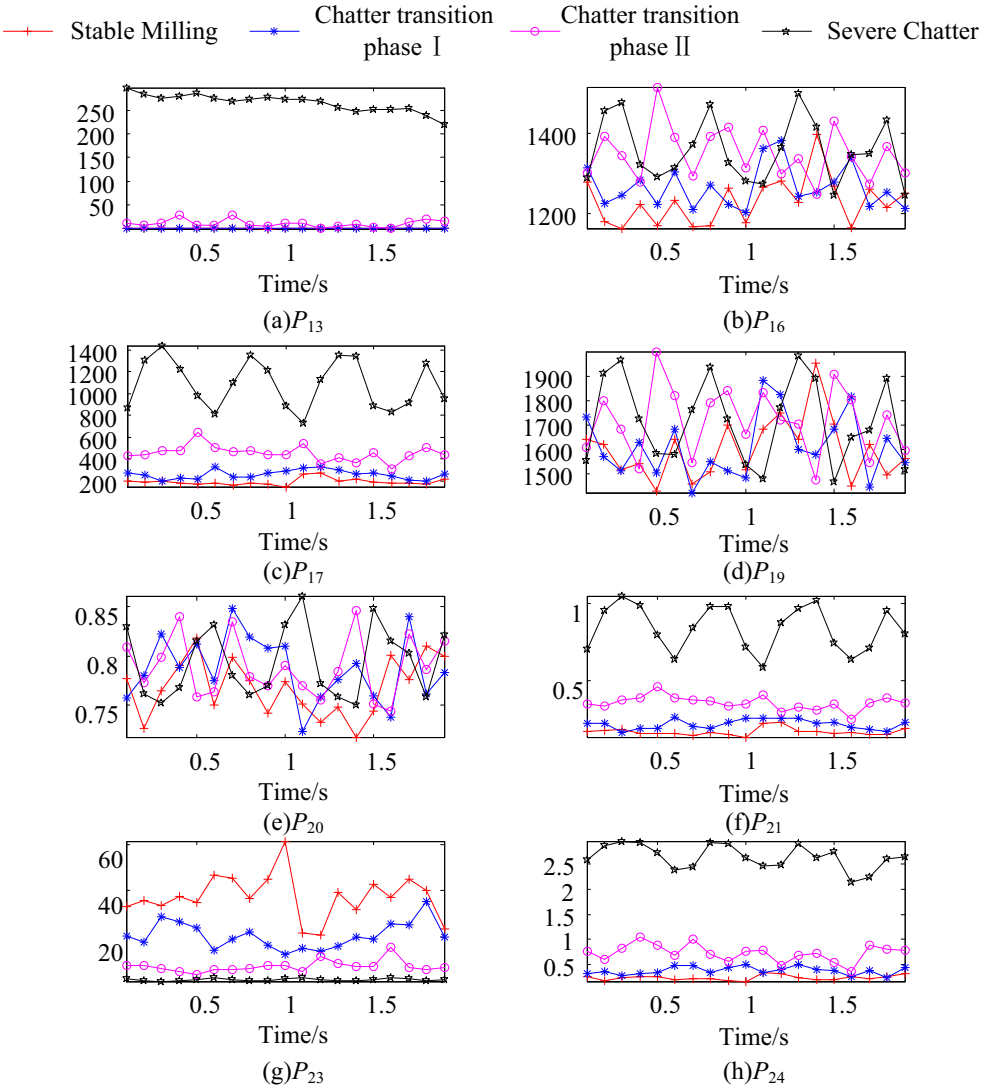

Fig. 9 Statistical indexes of the reconstructed signals in frequency domain. **a** P_{13}. **b** P_{16}. **c** P_{17}. **d** P_{19}. **e** P_{20}. **f** P_{21}. **g** P_{23}. **h** P_{24}

reflected by measuring the position of the main frequency band and the degree of frequency dispersion.

The commonly used statistical characteristic indexes in frequency domain are listed in Table 2, where $s_e(k)$ is the frequency spectrum of the reconstructed signal$x_e(n)$, Krepresents the number of spectral line,$k = 1, 2, \cdots, K$, and f_k is the frequency value of the$k$thspectral line. IndicatorsP_{16}, P_{19}, and P_{20} reflect the position change of the main frequency band, and indicatorsP_{13}, P_{17}, P_{21}, P_{23}, and P_{24} reflect the degree of dispersion or concentration of a spectrum.

4 Experiments

The equipment setup is shown in Fig. 3. The experiment was carried out in a three-axis vertical milling machine tool, and the highest speed of the spindle (Kessler DMS 080) can reach 24,000 r/min. Two PCB piezoelectric acceleration sensors with the sensitivity of 1000 mV/g, installed at the end of the spindle, are used to collect the vibration signal during the milling process. The experimental data are collected and stored by the AVANT MI-7008 Econ data acquisition system. Three kinds of tests were carried out, which are frequency

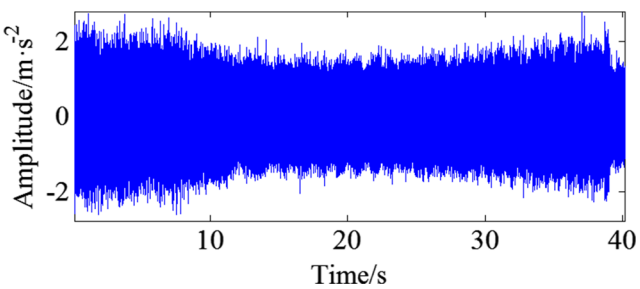

Fig. 10 The vibration signals during cutting

response function (FRF) test, statistical indicators selection, and cutting tests under variable depth of cut.

4.1 Frequency response function test

As the chatter frequencies appear near the low-order natural frequencies of the spindle-tool holder-tool (STT) system, it is necessary to test the FRF of the STT system to obtain the lower-order natural frequencies. The arrangement of the experimental equipment is shown in Fig. 4. The hammer is Kistler 9722 with the sensitivity of 12.85 mV/N; two acceleration sensors DYTRAN 3032A with the sensitivity of 10 mV/g are attached at the tool tip in the X and Y direction. Data acquisition and analysis are carried out by the modal analysis software of Econ data acquisition instrument, and the FRFs are shown in Fig. 5.

From the FRFs in Fig. 5a, b, it is concluded that the lower-order natural frequencies of the STT system in the X direction are 703.8, 1243, and 2006 Hz, and the lower-order natural frequencies in the Y direction are 725, 932, 1299, and 2028 Hz. Therefore, the sensitive frequency bands are defined as C_1 (700–950 Hz), C_2 (1150–1400 Hz), and C_3 (1900–2150 Hz).

4.2 Statistical indicators selection

The statistical indicators in Section 3 are verified with cutting tests to find the sensitive indicators. To simplify the problem, four typical cutting tests (i.e., stable milling, transition phase I of chatter, transition phase II of chatter, and severe chatter) were carried out, in which the depth of cut are 1, 2, 3, and 5 mm, respectively. All the cutting parameters are listed in Table 3.

The vibration signals are processed by the SST and TF filtering. The TF distribution and filtered TF distribution are shown in the Fig. 6. As the chatter becomes more severe, the energy at chatter frequencies becomes higher.

The filtered TF distribution is reconstructed based on SST, and the new time domain signal is obtained. Then, the statistical indexes in time domain are calculated according to Table 1, as shown in Figs. 7 and 8. Through the comparison in different states, root square amplitudeX_s and the root mean square value X_{rms}, absolute mean amplitudeX_a, and peak-to-peak value$X_p$are selected as indicators in time domain, which are sensitive to the chatter.

The statistical indexes in frequency domain are calculated in accordance with Table 3, and the results are shown in Fig. 9. P_{13}, P_{17}, P_{21}, and P_{24} are selected as the chatter indicators in frequency domain, which are more sensitive to the chatter information.

4.3 Cutting tests under variable depth of cut

The cutting tests under variable depth of cut were carried out to verify the effectiveness of the proposed method. The three-edge cemented carbide end milling cutter was used in this experiment, whose diameter is 10 mm. The workpiece is the thin-walled plate of 7075 aeronautical aluminum alloy, which is designed as right trapezoid to make the axial depth of cut continuously increase from 0 to 10 mm. The spindle speed is 10,200 r/min, feed per tooth is 0.01 mm/z, and the cutting width is 0.2 mm. The milling method is dry milling, and the direction is down milling. The vibration signal in the cutting process is shown in Fig. 10. From the signal in time domain, it is difficult to tell when the chatter occurs.

The vibration signals were processed with SST and the TF filtering method; the chatter indicators were extracted from the reconstructed signal in time domain and frequency domain. As the depth of cut increases, there is a transition from steady to chatter in milling process. The threshold for chatter detection is set based on 3σ criterion, that is, the threshold interval is$[\mu - 3\sigma, \mu + 3\sigma]$, where $\mu$is the mean value of the chatter indicator and σ is the standard deviation in stable milling state. During the cutting process, the value of indicators keeps

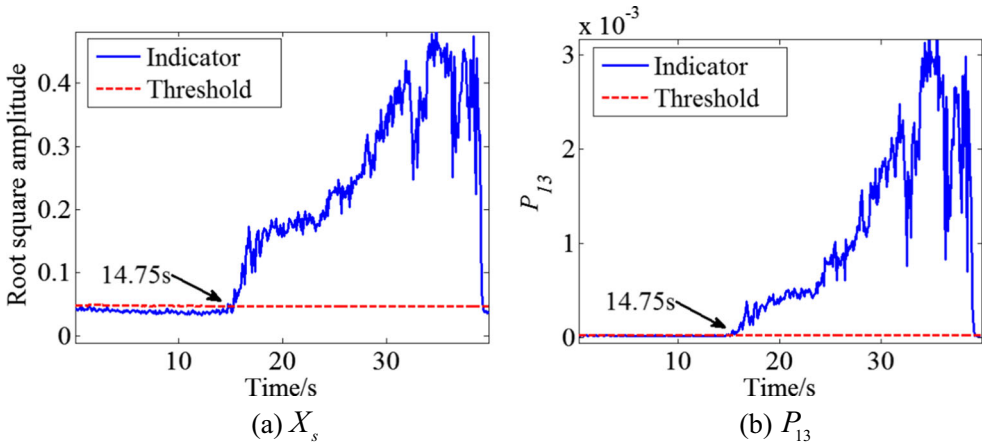

Fig. 11 The statistical indexes changes with time. **a** X_s and **b** P_{13}

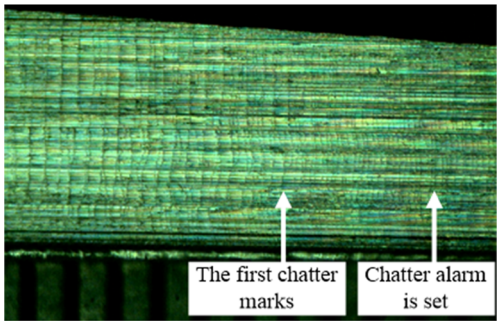

Fig. 12 The enlarged surface of workpiece machined in the first experiment

changing. If the indicator data is in the interval, the cutting state is stable; otherwise, chatter occurs.

In order to shorten the length of the paper, only two statistical indexes are shown, i.e., the root square amplitude$X_s$and P_{13} in frequency domain, as shown in Fig. 11.

The microscope MZDH0670 was used to observe the surface of the workpiece; the first obvious chatter mark in the chatter transition zone appears at about 65 mm, as shown in Fig. 12. Since the start time of cutting was 1.5 s and the feed rate was 288 mm/min, the time at the first chatter marks was about 15.04 s. Thus, the chatter was detected before severe marks were left on the workpiece.

In addition, the milling chatter experiments under different cutting width and feed per tooth were carried out respectively, and the experimental data of each group were analyzed. It is found that the proposed chatter detection method has good applicability in dealing with different conditions.

5 Conclusion

This paper presented a chatter detection method based on statistical indicators in milling process. The synchrosqueezing transform was used to preprocess the vibration signals. After the rearrangement of SST, the chatter energy aggregation was improved. The TF filtering was used to filter out the tooth passing frequency and its harmonics, which reduced the interference of these frequency bands and increases the proportion of the chatter frequencies, making the early weak chatter sign easier to be extracted. Eight statistical indexes were selected as chatter indicators from the reconstructed signal after TF filtering, including the root square amplitudeX_s, the root mean square value X_{rms}, absolute mean amplitudeX_a, and peak-to-peak valueX_p in time domain, as well as P_{13}, P_{17}, P_{21}, and P_{24} in frequency domain. The experimental results showed that the chatter can be detected successfully before severe chatter marks were left on the workpiece.

Acknowledgements The authors would like to acknowledge the support of the National Natural Science Foundation of China (No. 51575423, 51421004), the Natural Science Foundation of Shaanxi (No. 2017JM5120), and the Fundamental Research Funds for the Central University.

References

1. Cao H, Li B, He Z (2012) Chatter stability of milling with speed-varying dynamics of spindles. Int J Mach Tool Manu 52(1):50–58. https://doi.org/10.1016/j.ijmachtools.2011.09.004
2. Wan M, Ma Y-C, Zhang W-H, Yang Y (2015) Study on the construction mechanism of stability lobes in milling process with multiple modes. Int J Adv Manuf Technol 79(1–4):589–603. https://doi.org/10.1007/s00170-015-6829-4
3. Wan M, Feng J, Ma Y-C, Zhang W-H (2017) Identification of milling process damping using operational modal analysis. Int J Mach Tools Manuf 122:120–131. https://doi.org/10.1016/j.ijmachtools.2017.06.006
4. Wan M, Ma Y-C, Feng J, Zhang W-H (2016) Study of static and dynamic ploughing mechanisms by establishing generalized model with static milling forces. Int J Mech Sci 114:120–131. https://doi.org/10.1016/j.ijmecsci.2016.05.010
5. Wan M, Zhang W-H, Dang J-W, Yang Y (2010) A unified stability prediction method for milling process with multiple delays. Int J Mach Tools Manuf 50(1):29–41. https://doi.org/10.1016/j.ijmachtools.2009.09.009
6. Yang Y, Zhang W-H, Ma Y-C, Wan M (2016) Chatter prediction for the peripheral milling of thin-walled workpieces with curved surfaces. Int J Mach Tools Manuf 109:36–48. https://doi.org/10.1016/j.ijmachtools.2016.07.002
7. Cao H, Zhang X, Chen X (2017) The concept and progress of intelligent spindles: a review. Int J Mach Tool Manu 112:21–52. https://doi.org/10.1016/j.ijmachtools.2016.10.005
8. Tangjitsitcharoen S (2009) In-process monitoring and detection of chip formation and chatter for CNC turning. J Mater Process Technol 209(10):4682–4688. https://doi.org/10.1016/j.jmatprotec.2008.10.054
9. Liang M, Yeap T, Hermansyah A (2004) A fuzzy system for chatter suppression in end milling. Proc Inst Mech Eng B J Eng Manuf 218(4):403–417
10. Thaler T, Potočnik P, Bric I, Govekar E (2014) Chatter detection in band sawing based on discriminant analysis of sound features. Appl Acoust 77:114–121. https://doi.org/10.1016/j.apacoust.2012.12.004
11. Tangjitsitcharoen S, Saksri T, Ratanakuakangwan S (2013) Advance in chatter detection in ball end milling process by utilizing wavelet transform. J Intell Manuf 26(3):485–499. https://doi.org/10.1007/s10845-013-0805-3
12. Shih-Ming W, Ming-Je L, Sheng-Yu L, Hung-Wei L (2007) Application of wavelet transform on diagnosis and prediction of milling chatter. Chinese Journal of Mechanical Engineering 20(3)
13. Wang L, Liang M (2009) Chatter detection based on probability distribution of wavelet modulus maxima. Robot Comput Integr Manuf 25(6):989–998. https://doi.org/10.1016/j.rcim.2009.04.011
14. Yao Z, Mei D, Chen Z (2010) On-line chatter detection and identification based on wavelet and support vector machine. J Mater Process Technol 210(5):713–719. https://doi.org/10.1016/j.jmatprotec.2009.11.007
15. Chen B, Yang J, Zhao J, Ren J (2015) Milling Chatter prediction based on the information entropy and support vector machine. In, 2015. Atlantis Press,
16. Chin DH, Yoon MC (2005) Cutting force monitoring in the endmilling operation for chatter detection. Proc Inst Mech Eng B J Eng Manuf 219(6):455–465. https://doi.org/10.1243/095440505x32292

17. Cao H, Lei Y, He Z (2013) Chatter identification in end milling process using wavelet packets and Hilbert–Huang transform. Int J Mach Tools Manuf 69:11–19. https://doi.org/10.1016/j.ijmachtools.2013.02.007
18. Cao H, Zhou K, Chen X, Zhang X (2017) Early chatter detection in end milling based on multi-feature fusion and 3σ criterion. Int J Adv Manuf Technol. https://doi.org/10.1007/s00170-017-0476-x
19. Liu H, Chen Q, Li B, Mao X, Mao K, Peng F (2011) On-line chatter detection using servo motor current signal in turning. SCIENCE CHINA Technol Sci 54(12):3119–3129. https://doi.org/10.1007/s11431-011-4595-6
20. Fu Y, Zhang Y, Zhou H, Li D, Liu H, Qiao H, Wang X (2016) Timely online chatter detection in end milling process. Mech Syst Signal Process 75:668–688
21. Cao H, Zhou K, Chen X (2015) Chatter identification in end milling process based on EEMD and nonlinear dimensionless indicators. Int J Mach Tools Manuf 92:52–59. https://doi.org/10.1016/j.ijmachtools.2015.03.002
22. Sun H, Zhang X, Wang J (2016) Online machining chatter forecast based on improved local mean decomposition. Int J Adv Manuf Technol 84(5–8):1045–1056. https://doi.org/10.1007/s00170-015-7785-8
23. Daubechies I, Lu J, H-T W (2011) Synchrosqueezed wavelet transforms: an empirical mode decomposition-like tool. Appl Comput Harmon Anal 30(2):243–261. https://doi.org/10.1016/j.acha.2010.08.002
24. Cao H, Yue Y, Chen X, Zhang X (2017) Chatter detection in milling process based on synchrosqueezing transform of sound signals. Int J Adv Manuf Technol 89(9–12):2747–2755. https://doi.org/10.1007/s00170-016-9660-7